

Response of Plasma-Polymerized Hexamethyldisiloxane Films to Aqueous Environments

Journal Article**Author(s):**

Blanchard, Noemi E.; Naik, Vikrant V.; Geue, Thomas; Kahle, Olaf; [Hegemann, Dirk](#) ; Heuberger, Manfred

Publication date:

2015-12-01

Permanent link:

<https://doi.org/10.3929/ethz-b-000107981>

Rights / license:

[In Copyright - Non-Commercial Use Permitted](#)

Originally published in:

Langmuir 31(47), <https://doi.org/10.1021/acs.langmuir.5b03010>

Response of Plasma-Polymerized Hexamethyldisiloxane Films to Aqueous Environments

Noemi E. Blanchard,^{†,‡} Vikrant V. Naik,[‡] Thomas Geue,[§] Olaf Kahle,^{||} Dirk Hegemann,[†] and Manfred Heuberger^{*,†,‡}

[†]Empa, Swiss Federal Laboratories for Materials Science and Technology, 9014 St. Gallen, Switzerland

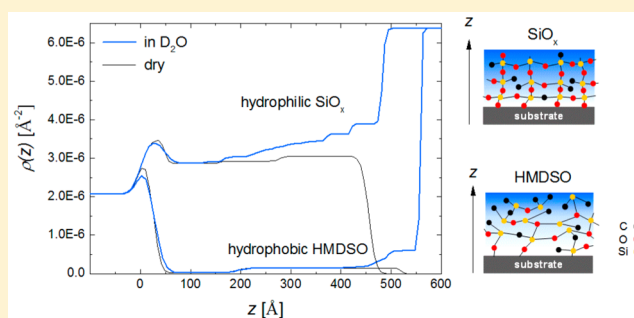
[‡]Laboratory for Surface Science and Technology, Department of Materials, ETH Zurich, 8093 Zürich, Switzerland

[§]Laboratory for Neutron Scattering and Imaging, Paul Scherrer Institut, 5232 Villigen, Switzerland

^{||}Fraunhofer Research Institution for Polymeric Materials and Composites PYCO, 14513 Teltow, Germany

Supporting Information

ABSTRACT: Thin plasma polymer films were deposited in hexamethyldisiloxane (HMDSO) and HMDSO/O₂ low-pressure discharges and their chemical structures analyzed using infrared (IR) spectroscopy and neutron reflectometry (NR). The (plasma-polymerized) ppHMDSO film exhibits hydrophobic, poly(dimethylsiloxane)-like properties, while the retention of carbon groups is reduced by O₂ addition, yielding a more inorganic, hydrophilic ppSiO_x film. Both films show a minor (vertical) density gradient perpendicular to the substrate, where the exposed film surface seems to be more oxidized, indicating oxidative aging reactions upon contact with air. The hydration and water uptake abilities of the films in aqueous environments were investigated in humid environments using ellipsometry, NR in D₂O, and multiple transmission-reflection IR measurements after equilibration of the films in water.



1. INTRODUCTION

Thin films prepared via plasma polymerization are suitable for a wealth of applications, including protective and/or barrier coatings, as well as sensor or biomedical applications.¹ In addition, plasma polymerization offers the possibility of tuning film properties such as hardness, elastic modulus, wettability, and chemical composition by accurately controlling the energetic conditions in the plasma gas phase and at the substrate surface.^{2–5} In comparison to conventional polymers, plasma polymers are more branched and cross-linked and contain additional chemical structural elements not found in conventional polymers.^{6–8} Hexamethyldisiloxane (HMDSO) is widely used as a precursor monomer for plasma polymerization due to its suitable vapor pressure and nontoxicity. Moreover, depending on the deposition conditions and progressive admixture of reactive gases, such as oxygen, the obtained film properties range from hydrophobic, poly(dimethylsiloxane)-like (PDMS-like) to more hydrophilic and nanoporous and finally to more inorganic hard films that are based on a stable Si–O–Si backbone containing only a small amount of residual hydrocarbon groups. It is thus not surprising that plasma-polymerized HMDSO films are used in rather diverse applications such as antibacterial nanosilver composite materials, pervaporation membranes, humidity sensors, hydrophobic protective coatings, or barrier films.^{9–17} In numerous applications, the plasma polymer films prepared from HMDSO are in contact with water and,

depending on the specific application, need to meet special requirements regarding film stability and film hydration (i.e., penetration of water into the films): a hydrophobic protective film should keep its water-repelling properties over long time periods, while for antibacterial applications water needs to diffuse through the plasma polymer matrix to hydrate and leach silver ions, which provide the antibacterial effect. While many studies report the long-term functionality of the respective applications,^{10–12,14} only a few directly investigate the response of plasma-polymerized HMDSO films in aqueous environments.^{10,18} Water migration in polymer films is affected by many factors such as the porosity, film chemistry, or mechanical properties of the film. Models describing the diffusion of water in such systems are thus often highly system-specific and complicated by the different mechanisms involved (pore filling in the cross-linked film, adsorption of water at the pore walls, and diffusion of water molecules through the network of interconnected nanometer-sized voids).^{19–23} In addition, siloxane bonds present in HMDSO films can hydrolyze in the presence of water, creating hydrophilic Si–OH groups, further facilitating the migration of water in the films, which thus leads to a concentration-dependent reactive diffusion.^{24–26}

Received: August 12, 2015

Revised: October 5, 2015

Published: October 9, 2015

Neutron reflectometry (NR) is a technique that is sensitive to fluctuations of the scattering length density (SLD) normal to the surface and is suitable to investigate thin films. Moreover, the possibility of increasing contrast between the film and the solution by deuteration makes this method well suited to study the penetration of deuterated water into thin plasma-polymerized HMDSO films. Nelson et al.¹⁸ have investigated hydrophilic allylamine (AA) and hydrophobic HMDSO plasma polymer films using neutron reflectometry and showed that the AA-derived film swells considerably in D₂O, while the HMDSO-derived film was found to be essentially impermeable to deuterated water. The same group also conducted a similar study with plasma polymers containing reactive amines, in which they showed that a small change in monomer composition (heptylamine vs allylamine) results in quite different cross-linking degrees as well as different water uptakes and functional group retentions.²⁷ In other neutron reflectometry studies, the influence of the deposition conditions on the film properties and efficacy against protein fouling of plasma-polymerized PEG-like films was investigated⁷ or the microstructure of plasma-polymerized methyl methacrylate was characterized.²⁸ In this work, a selection of two sufficiently different and previously well characterized plasma polymer films were deposited from the HMDSO monomer with and without an admixture of oxygen⁵ and further characterized in air using neutron reflectometry and IR measurements. The hydration of the two films in aqueous environments was studied in situ with neutron reflectometry. Additional IR measurements after the equilibration of the films in water have been performed and compared to the NR results.

2. EXPERIMENTAL SECTION

2.1. Plasma Polymerization. The plasma polymers were deposited in a capacitively coupled, rf-driven ($f = 13.56$ MHz) reactor described in detail elsewhere.⁵ For this study, two different films were deposited identically to two selected established protocols in refs 5 and 29, that is (i) a SiO:CH film deposited from a HMDSO discharge, henceforth called the “ppHMDSO” film, and (ii) a SiO_x film deposited from a plasma with a fixed oxygen-to-HMDSO-ratio of 10:1 and a significantly reduced carbon content, henceforth referred to as the “ppSiO_x” film. The hexamethyldisiloxane monomer was purchased from Fluka, and the HMDSO-containing tank, including the tubing, was stabilized at a temperature of 43 °C outside the reactor. The HMDSO total gas flow rate was kept constant at 4 sccm using a thermostabilized mass flow controller (also at 43 °C). For both deposition conditions, argon (20 sccm) was added as the carrier gas. Oxygen and argon were purchased from Carbagas, Switzerland. The gases were mixed outside the plasma chamber and introduced via the same gas shower. The process pressure was fixed at 7 Pa. The ppHMDSO and the ppSiO_x films were deposited using power inputs of 50 and 100 W, yielding negative self-bias voltages of 70 and 110 V at the rf electrode, respectively. Prior to deposition of plasma polymer films, the substrates were precleaned in Ar/O₂ plasma (80 sccm/20 sccm). For neutron reflectometry measurements, identical films were deposited onto double-side-polished silicon blocks (<100>, dimensions 1 cm × 5 cm × 10 cm, SPM, Liechtenstein), while for IR measurements double-side-polished silicon wafers (<111>, Si-Mat, Germany) were used as substrates. To coat the silicon blocks, a special sample holder was designed, ensuring that the coating conditions at the block surface were homogeneous and identical to those at the rf electrode (mainly by embedding the block into the rf electrode). The films used for ellipsometry measurements were deposited onto silicon wafers. Reference glass slides and silicon wafers were coated to determine the deposition rate and the film density. The deposited mass was determined by weighing the glass slides directly before and after the deposition process. The film thickness was measured over a masked film edge with a profilometer (Veeco, Dektak 150). The film density was then calculated from the volume and the mass of the coatings.

2.2. Neutron Reflectometry. Neutron reflectometry measurements were performed using the AMOR reflectometer at the Swiss Spallation Neutron Source (SINQ) at the Paul Scherrer Institut (PSI), Villigen, Switzerland.³⁰ The reflectometer was operated in a time-of-flight mode covering a wavelength range of $\lambda = 0.35$ –1.2 nm, and the reflectivity was recorded at three angles of incidence (0.5°, 1.5°, and 3.2°). Because AMOR is an energy-dispersive instrument, the reflectivity could be obtained in a q_z range of $0.01 \text{ \AA}^{-1} \leq q_z \leq 0.19 \text{ \AA}^{-1}$, where q_z is the magnitude of the momentum transfer vector \vec{q} , $q_z = (4\pi/\lambda) \sin \theta$. The reflectivity R of the sample was obtained by dividing the intensity of the reflected beam by the intensity of the incoming beam and normalizing to 1. For the measurements in solution, deuterated water (Sigma-Aldrich, 99.9 atom % D) was used instead of “normal” water due to the larger SLD of D₂O ($\rho = 6.366 \times 10^{-6} \text{ \AA}^{-2}$) compared to H₂O ($\rho = -5.610 \times 10^{-7} \text{ \AA}^{-2}$), providing better contrast between the film and the penetrating solution. The coated silicon substrates were mounted in a liquid cell connected to a cooling/heating system. Each of the investigated films was measured four times: first in the dry state (i.e., against air), then in D₂O at 20 °C, a third time after the system was equilibrated for 3 h at 60 °C, and finally again at 20 °C after the system was allowed to cool to reach stable conditions.

The data were modeled using the Parratt formalism³¹ with the Parratt32 program.³² The data were fitted as $\log R$ vs q_z using a multilayer model, which includes the silicon block, the native SiO₂ layer, the plasma polymer, and the surrounding medium (air or D₂O). If necessary, the plasma polymer layer was subdivided into several layers to approximate a vertical SLD gradient. The SLDs used in the models for Si, SiO₂, and D₂O were 2.073×10^{-6} , 3.476×10^{-6} , and $6.366 \times 10^{-6} \text{ \AA}^{-2}$, respectively. To approximate smooth gradients, up to eight equidistant SDL layers were initially set; in this case the (dependent) parameters were fitted groupwise to limit the number of degrees of freedom.

2.3. IR Measurements. Multiple transmission–reflection (MTR) FTIR measurements were performed on a home-built MTR setup (Prof. Shoujun Xiao, University of Nanjing, China).³³ The double-side-polished Si wafer was placed between two gold mirrors, 2 mm apart, such that its distances from the two mirrors were 0.3 and 1.2 mm, and the simplified number of transmission passes was six. Only one side of the wafer was coated with the plasma polymer film. The spectra were acquired on a Bruker IFS66v FTIR spectrometer in vacuum at a resolution of 4 cm^{-1} , measured using a mercury cadmium telluride (MCT) detector, which was cooled by liquid nitrogen. A bare, plasma-cleaned (conditions as described above) Si wafer was used as the background. Each sample and background measurement consisted of 256 scans. The enhanced sensitivity provided by this method allows just for the study of very thin films as produced in this work. The films were measured with minimal delay after equilibration in deionized water for 3 weeks (at room temperature).

2.4. Ellipsometry. Ellipsometric measurements were performed on a spectroscopic ellipsometer (SE850) from Sentech Instruments equipped with a humidity chamber. The humidity is controlled by mass flow controllers; the humidity range is limited to values between 2% and 80% relative humidity. The incident angle is fixed to 70°. The ellipsometer software is adapted to control and record the humidity. The thickness of the investigated films was 100 ± 5 nm. The films were equilibrated at minimum humidity for 30 min before the humidity-dependent measurements began. The humidity–time profile was as follows: ramping from 2% to 80% relative humidity in 40 min, holding at maximum humidity for 4 h, ramping down to 2% humidity in 40 min, and holding at minimum humidity for 4 h. Measurements were performed every 2 min; i.e., 280 ellipsometric measurements were made for one complete humidity cycle. The measured ellipsometric angles Ψ and Δ were converted to the thickness d and the (dispersion of) refractive index n by a fitting process using a simple ellipsometric layer model consisting of the silicon substrate, the native SiO₂ layer, and the plasma polymer film. The optical properties of the Si wafer layer and the 2 nm thick native SiO₂ layer are described by literature data. The plasma polymer layer (HMDSO or SiO_x) was fitted to the Sellmeier equation.³⁴ A wavelength range from 360 to 800 nm was used. A single value for n is calculated at $\lambda = 589$ nm. Combining n and d allows the calculation of a

relative mass of the layer; i.e., with ellipsometric investigations, changes in the relative mass of the film, Δm_{rel} (e.g., by water uptake), can be determined, where $\Delta m_{\text{rel}} = (m - m_0)/m_0$, with m_0 representing the initial mass.

3. RESULTS AND DISCUSSION

In this study, two plasma polymer films deposited from the same precursor, namely, HMDSO, with or without an admixture of oxygen to the plasma process, have been studied with respect to their chemical structure and response to aqueous environments. Both the ppHMDSO film and the ppSiO_x film are identical to two previously characterized films.⁵ The film properties relevant here are briefly summarized in Table 1.

Table 1. Film Properties of HMDSO- and HMDSO/O₂ (1:10)-Derived Plasma Polymer Films (in the Dry State)

	O/Si	C/Si	film density (g cm ⁻³)	contact angle (deg)
ppHMDSO	0.93 ± 0.01	1.87 ± 0.02	1.24 ± 0.02	102 ± 1
ppSiO _x	1.91 ± 0.02	0.49 ± 0.01	1.89 ± 0.02	72 ± 2

The reported atomic ratios reveal that the ppHMDSO film is rather PDMS-like, comprising mainly methyl groups and additional cross-linking by methylene groups, while increasing the power and the addition of oxygen to the process yields films with a more inorganic character.^{4,35} However, the examined ppSiO_x film still retains a significant amount of hydrocarbon groups (besides silanol groups), ensuring a certain porosity and hydration within the films.^{5,26,36} To assess the vertical density profile of these plasma polymer films in the dry and hydrated states, neutron reflectometry measurements were performed. Neutrons are well suited to investigate polymer films because they interact with the atomic nuclei and thus provide a good contrast also for lighter atoms. In addition, the possibility to increase this contrast by using deuterated water further helps to study the changes in the vertical density profile of the films when in contact with D₂O.

3.1. Characterization of Dry Films. Typical neutron reflectivity curves of ppHMDSO and ppSiO_x films measured

against air (i.e., in the dry state) are shown in Figure 1a. The observed oscillations are Kiessig fringes³⁷ that arise due to the interference of neutrons reflected at the polymer/air and polymer/substrate interfaces, respectively. The periodicity of these Kiessig fringes is characteristic for the total thickness of the polymer film, while their amplitude is related to the contrast at the interfaces.³⁸

A layer model composed of the silicon substrate, the native SiO₂ layer, the plasma polymer layer, and the respective medium was assumed for fitting. Modeling the plasma polymer as a single layer of uniform density did not yield satisfying fitting results as shown by the inset in Figure 1a, indicating that the films do not exhibit a perfectly homogeneous density perpendicular to the surface. The dry plasma polymer films were thus approximated by three layers of variable thickness and SLD to account for this minor density gradient. The scattering length density profiles resulting from the best fits to the experimental data are shown in Figure 1b, and the resulting fit parameters are reported in Table 2. The dry ppHMDSO film exhibits scattering length densities

Table 2. Neutron Reflectivity Fitting Results of the Two HMDSO- and HMDSO/O₂ (1:10)-Derived Plasma Polymer Films

	SLD, ρ (10 ⁻⁶ Å ⁻²)	thickness, d (Å)	transition width, σ (Å)
ppHMDSO		496	
SiO ₂		24	14
layer 1	0.02	167	12
layer 2	0.14	190	14
layer 3	0.15	139	5
ppSiO _x		406	
SiO ₂		49	14
layer 1	2.86	109	6
layer 2	2.93	119	5
layer 3	3.05	178	8

from 0.02×10^{-6} to 0.15×10^{-6} Å⁻², which are similar to the SLD of PDMS,³⁹ in agreement with the PDMS-like character of this film. These SLDs present a weak contrast to air, resulting in

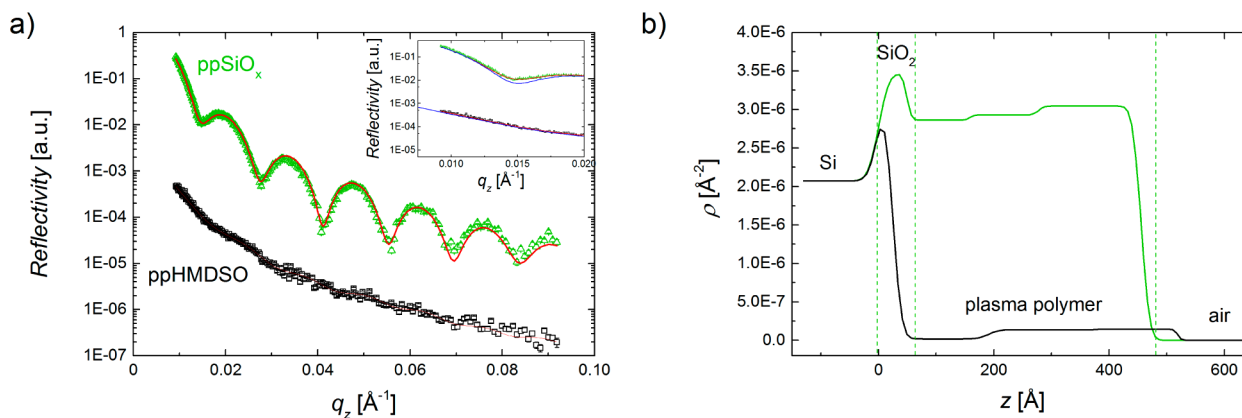


Figure 1. (a) Neutron reflectivity of plasma polymer films in the dry state. Experimental data are shown as green open triangles (ppSiO_x) and black open squares (ppHMDSO). The solid red lines represent the best fits to the experimental data (χ^2 (ppHMDSO) = 1.19×10^{-2} , χ^2 (ppSiO_x) = 2.63×10^{-2}). The ppHMDSO data are vertically shifted by a factor of 10^{-2} for the sake of clarity. The inset shows an enlargement of the low- q_z range, including reflectivity curves resulting from a single-layer model (blue lines; χ^2 (ppHMDSO, one layer) = 2.89×10^{-2} , χ^2 (ppSiO_x, one layer) = 3.77×10^{-2}). (b) Scattering length density profiles resulting from the best fits shown in (a) as a function of the layer depth z , where the origin of the z -axis is set at the Si/SiO₂ interface. The dashed vertical lines indicate the location of the Si/SiO₂, SiO₂/film, and film/air interfaces. The transition width between layers is also a fitting parameter.

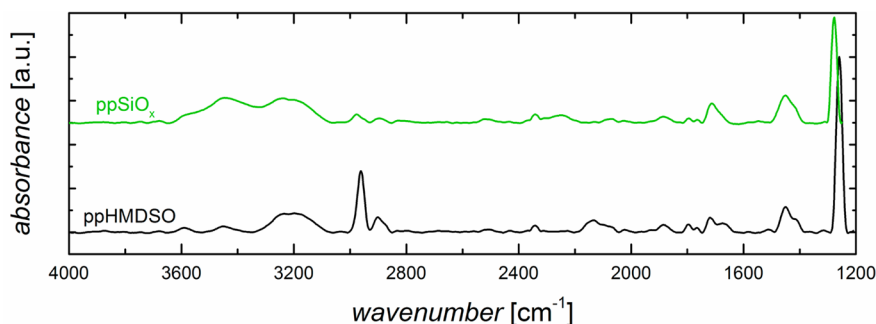


Figure 2. IR spectra of the freshly deposited films. Curves are shifted vertically for clarity.

Kiessig oscillations of low amplitude in the neutron reflectivity. On the other hand, the SLD of the dry ppSiO_x film gradually goes from $2.86 \times 10^{-6} \text{ \AA}^{-2}$ close to the silicon substrate to $3.05 \times 10^{-6} \text{ \AA}^{-2}$ at the film/air interface. This film thus provides a good contrast to air, and therefore, the Kiessig fringes are of higher amplitude. Due to the different contrasts of the two films, also the deviations of the unsatisfactory one-layer fit in the inset of Figure 1a seem less pronounced for the ppHMDSO film than for the ppSiO_x film.

Pre-cleaning of the substrate in an Ar/O₂ plasma leads to rather thick native silicon dioxide layers of 2.4 and 4.9 nm, respectively, i.e., thicker in the case of the O₂ admixture during film deposition. The roughness of the film surface is in accordance with values previously reported from atomic force microscopy (AFM) measurements.^{2,40,41} For smoothing of the otherwise abrupt change of SLD from one layer to the next in the fitting model, we used the transition width parameter, σ . Typical values of 10–20 Å were attained in our fits, which are 15–30% of the film thickness. We note that a sharp transition ($\sigma = 0$) of a laterally rough interface cannot be distinguished from a smooth transition ($\sigma > 0$) by reflectivity measurements.⁴² The small gradient of the scattering length density fitted here is different from the result of Nelson et al., who observed a homogeneous density for an HMDSO film.¹⁸ We cannot exclude that the vertical gradient was induced by postdeposition aging reactions upon contact with air, as it was not possible to measure the films in situ immediately after the deposition. The relatively harsh plasma conditions (ion bombardment and vacuum ultraviolet (VUV) radiation) introduce free radicals within the film that can further react with ambient oxygen or water, leading to a delayed formation of silanol, carbonyl, and siloxane groups and a decrease of Si–H within the film.^{43,44} These reactions lead to an overall higher oxygen and lower hydrogen content and thus to an increase of the SLD for neutron scattering. As these aging reactions depend on diffusion of oxygen (and water) into the films,⁴⁴ the degree of aging is expected to decrease from the film surface toward the substrate, resulting in a minor vertical SLD gradient.

The IR spectra of the plasma polymer films measured shortly after deposition are presented in Figure 2. Characteristic peaks were assigned according to literature data.^{8,45,46} The ppHMDSO spectrum exhibits several characteristic peaks revealing the PDMS-like structure of this film: asymmetric (2960 cm^{-1}) and symmetric (2905 cm^{-1}) CH₃ stretching, asymmetric (1410 cm^{-1}) and symmetric (1260 cm^{-1}) CH₃ bending in Si–(CH₃)_x with $x = 1, 2, 3$. The position of this rightmost peak depends on the degree of oxidation of the Si environment and shifts to higher wavenumbers for higher oxidation states.^{47,48} In addition to these peaks, the spectrum of the plasma-polymerized film also exhibits the following peaks: Si–CH₂–Si (1355 cm^{-1}), CH_x bending

(1455 cm^{-1}), C=O (1710 cm^{-1}), Si–H (2130 cm^{-1}), and –OH (around 3200 cm^{-1}). In the spectrum of the ppSiO_x film, also shown in Figure 2, the peaks related to methyl groups (CH₃ stretching and bending) are significantly less intense—indicating the lower retention of methyl groups. Additionally, several peaks are shifted to higher wavenumbers, confirming the stronger cross-linking and more oxidized Si environment:^{47,49–51} the peak related to CH₃ symmetric bending in Si–(CH₃)_x (1277 cm^{-1}), the Si–H stretching vibration (2248 cm^{-1}), and the CH₃ asymmetric stretching (2975 cm^{-1}). Also, the C=O peak and the peak around 1450 cm^{-1} (resulting from an overlap of several CH_x bending and/or scissoring vibrations) are more intense and broader, confirming the stronger cross-linking of this film. The intensity of the –OH band is higher and broadened, exhibiting an additional peak around 3400 cm^{-1} attributed to water or highly associated hydroxyl groups.^{36,52} It should be noted here that the region below about 1800 cm^{-1} is difficult to interpret for two reasons: (1) In organosilicon plasma polymers, many chemical bonds such as CH_x, Si–C-related bonds, C=O, and C=C show vibrations in this region which may overlap,⁴⁶ and in addition, the position of some of these vibrations is dependent on the electronegativity of the surroundings. This complicates an accurate peak assignment. (2) As the films are deposited on silicon wafers, the Si–O–Si stretching vibration around 1050 cm^{-1} (see the Supporting Information), to which not only the film but also the substrate contributes, results in a broad and very intense peak. This band dominates the measured spectrum and also the background in this region,^{17,53} which makes direct comparison of peak intensities difficult. Indeed, in the literature this region of the spectrum is often either not commented on, even if some features are clearly visible, or not shown at all.^{17,41,45,51,53–56}

Overall, using the information about film density, the structural film composition as determined by IR measurements, and the chemical surface composition as determined by XPS, the measured scattering length density can be readily reproduced with the aid of the NIST SLD calculator⁵⁷ by adjusting the film composition until the calculation matches the experimentally observed SLD. It was thereby assumed that the chemical composition as determined by XPS measurements corresponds to the composition of the outermost layer (i.e., layer 3). For the ppHMDSO film, the composition reported by Nelson et al. for a similar film¹⁸ was used as a starting point. In addition, on the basis of the IR spectrum, it was assumed that the majority of hydrogen atoms present in the film are present as CH₃. The as-obtained film composition for the outermost layer was Si₆₈O₆₃C₁₃₁H₃₇₉. To account for the aging reactions reported above, a higher hydrogen content and a ~5% lower O/Si ratio were assumed for the innermost layer, resulting in a film

composition of $\text{Si}_{68}\text{O}_{56}\text{C}_{131}\text{H}_{392}$. For the ppSiO_x film the following film compositions were derived: $\text{Si}_{68}\text{O}_{130}\text{C}_{34}\text{H}_{21}$ for the film/air and $\text{Si}_{68}\text{O}_{126}\text{C}_{34}\text{H}_{38}$ for the Si block/film interfaces, respectively. The so-determined film compositions are somewhat ambiguous (mainly regarding the exact H content). However, here these compositions should serve more as an estimate of the fraction of hydrogen atoms retained within the films than as exact film compositions. In combination with the independently determined film parameters (density, chemical structure, and composition), this estimate seems consistent and yields values of H/C of 2.9 to almost 3 (which is reasonable considering the PDMS-like film properties) for the ppHMDSO film and a H/C ratio of 0.6–1.1 for the ppSiO_x film. Even if roughly 5–10% of silanol group formation might be assumed by hydration and silica hydrolysis, it can be stated that the ppSiO_x film reveals significantly reduced overall hydrogen content compared to ppHMDSO.³⁶

3.2. Response of Plasma Polymer Films to Aqueous Environments. Ellipsometry measurements of the two plasma polymer films confirm that the ppSiO_x film behaves differently in a humid environment than the ppHMDSO film, as illustrated in Figure 3, where we report the relative change in mass upon an

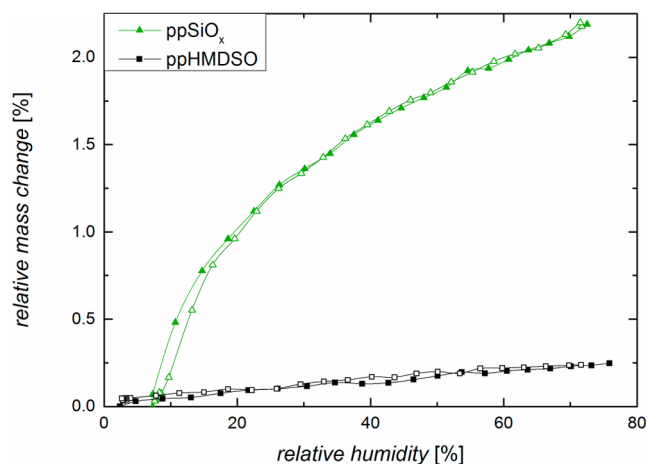


Figure 3. Progress of the relative change in mass for the ppSiO_x (green triangles) and ppHMDSO (black squares) films measured by ellipsometry as a function of the relative humidity. Filled symbols represent increasing relative humidity; open symbols represent decreasing relative humidity.

increase in relative humidity. The increase in relative mass is more pronounced for the ppSiO_x film ($\sim 2.2\%$) than for the ppHMDSO film ($\sim 0.25\%$). In addition, the ppSiO_x film seems to exhibit a slight hysteresis (as seen by the deviation of the open triangles from the filled triangles for humidity lower than 25%). It is also observed that the change in relative mass is nearly instantaneous (within a few minutes) and that no change occurs over extended times when the humidity is held constant at 80% (data not shown). This raises the question of whether the observed increase in mass is due to the formation of a water layer on top of the films or rather due to the penetration of water into the films. To discriminate surface film condensation from water penetration, additional NR measurements have been realized with both films immersed in liquid (where no water layer can be formed on top of the samples).

The behavior in an aqueous environment of the two different films was studied by neutron reflectivity measurements in D_2O at room temperature (20 °C) and at an elevated temperature (60

°C). The measurement at elevated temperature was performed to investigate the effect of the water surface tension on the degree of solvent penetration. Increasing the temperature to 60 °C decreases the surface tension of D_2O by about 10%, which might facilitate D_2O penetration into the films, as the energetic barrier presented by the hydrophobic groups can be overcome more easily by a solvent with lower surface tension. For comparison, the contact angle of water on the examined ppHMDSO plasma polymer film was found to vary between 102° and 75°, depending on the water exposure time.⁵ Similarly, the water contact angle on the ppSiO_x film varies between 72° and 50° upon immersion in water. A second measurement at 20 °C was repeated afterward to investigate the reversibility of the respective plasma polymer/ D_2O system. In the NR fitting models for the films measured in D_2O , the thickness and transition width of the SiO_2 layer were fixed to the values obtained for the fitting of the dry films, but to obtain a satisfying agreement between the fit and the experimental data, more layers had to be added (see also the Supporting Information). In the case of the ppSiO_x film depicted in Figure 4a, the plasma polymer layer including hydration water was best approximated by eight similarly thick sublayers. The eight layers were used to mimic a smooth gradient, where the thickness of the layers was initially equidistant, but then variable during the fitting procedure. The SLD of each layer was allowed to fully vary within the limiting bounds of the SLDs of the plasma polymer film and D_2O to account for possible solvent penetration. The resultant scattering length density profiles are presented in Figure 4b, and the obtained fitting parameters are reported in Table 3. After fitting, a consistent gradual increase of the scattering length density toward the film surface can be observed for all measurements. In addition, the ppSiO_x film apparently swells by about 7% compared to the dry state, and its thickness increases slightly from 434 to 438 Å with the immersion time in D_2O .

The reflectivity of the ppHMDSO film is shown in Figure 4c. The fitted model SLD with the smallest χ^2 was achieved with a structured model consisting of six individual layers: two thicker layers close to the silicon block and four thinner layers at the film surface. Again, the thickness and SLD of each layer were allowed to vary in the fit to accommodate possible solvent penetration. The SLD profiles resulting from the best χ^2 fits to the data are shown in Figure 4d. Upon immersion of the film in D_2O at 20 °C, an increase in SLD at the film surface can be noted, while the SLD close to the silicon substrate remains similar to that of the dry polymer. The ppHMDSO film swells by an amount similar to that of the ppSiO_x film relative to the dry state. At 60 °C we observe a pronounced increase of the scattering length density in the outermost layer and only a slight increase in the inner layers. The SLD profile fitted after the second measurement at 20 °C is almost identical to the SLD profile obtained for the first measurement at this temperature, indicating reversibility of the hydration process.

Note that an increased scattering length density might also result from hydrogen exchange with deuterium (from D_2O) during the measurement. The lower hydrogen content in ppSiO_x , however, limits this effect, leaving much stronger water penetration of the more hydrophilic, nanoporous film compared to ppHMDSO.

The approximation of gradients via multiple layers used here obviously leads to a higher number of (dependent) fitting parameters; we stress however that the groupwise fitting practiced here resulted in reliable convergence (see also the χ^2 values reported in the Supporting Information). Nevertheless,

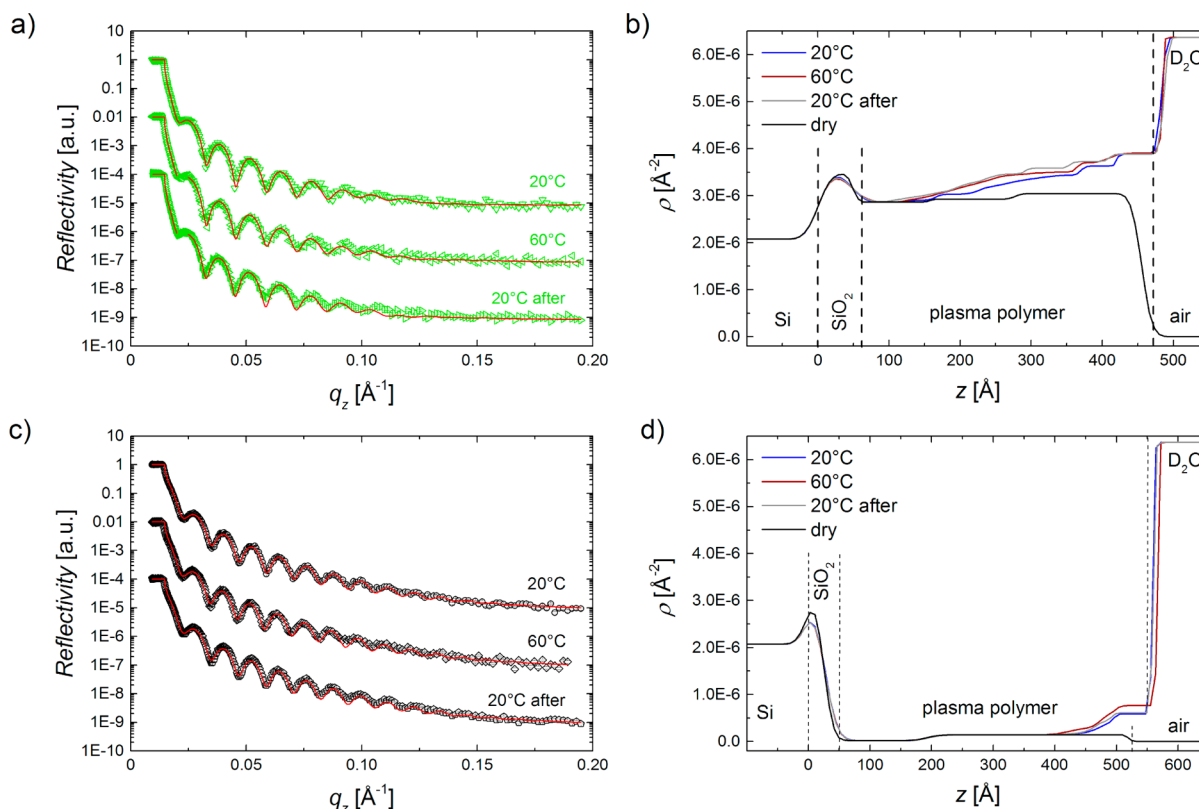


Figure 4. Neutron reflectivity of ppSiO_x (a) and ppHMDSO (c) films measured in D₂O at different temperatures. Experimental data are shown as symbols, while the solid red lines represent the best fits (χ^2 values are listed in the Supporting Information). The data sets for different temperatures are shifted vertically for the sake of clarity. Scattering length density profiles for the ppSiO_x (b) and ppHMDSO (d) films as a function of the layer depth z , where the origin of the z -axis is set at the Si/SiO₂ interface. The dashed vertical lines indicate the location of the Si/SiO₂, SiO₂/film, and film/medium interfaces.

Table 3. Parameters Resulting from the Best χ^2 Fits to the Neutron Reflectivity Data Recorded at Different Temperatures in D₂O^a

		20 °C			60 °C			20 °C after		
		d	ρ	σ	d	ρ	σ	d	ρ	σ
ppSiO _x		434			436			438		
	layer 1	75	2.86	14	73	2.86	18	67	2.86	16
	layer 2	41	2.91	10	36	2.91	5	39	2.99	18
	layer 3	61	3.03	6	42	3.07	18	39	3.06	10
	layer 4	44	3.19	12	46	3.26	20	45	3.27	14
	layer 5	50	3.36	22	59	3.45	17	53	3.47	14
	layer 6	50	3.44	21	61	3.51	19	63	3.59	5
	layer 7	50	3.63	5	46	3.70	5	55	3.73	5
ppHMDSO	layer 8	63	3.88	3	73	3.91	13	77	3.88	5
		535			541			537		
	layer 1	169	0.02	17	169	0.02	17	170	0.02	17
	layer 2	190	0.14	16	190	0.14	16	190	0.14	16
	layer 3	38	0.15	16	39	0.15	16	35	0.15	16
	layer 4	52	0.17	16	52	0.29	20	47	0.18	10
	layer 5	22	0.44	17	24	0.62	12	28	0.47	14
	layer 6	63	0.59	5	67	0.77	7	67	0.62	5

^aThe thickness d and transition width σ of the layers are given in angstroms, and the SLD ρ is given in 10^{-6} \AA^{-2} . The total thickness of the films is also indicated for each measurement.

additional ellipsometry measurements in a humid environment as well as more IR measurements of the films in deionized water were performed to independently verify the hydration of the films observed with fitting of the NR data. Figure 5 shows the IR spectra after equilibration in water in comparison to the freshly prepared dry films.

The main differences between the spectra measured in the dry and hydrated states can be observed in the OH region (3000–3800 cm^{-1}). For the ppSiO_x film the intensity of the OH band increases; especially the peak around 3400 cm^{-1} attributed to additional highly associated hydroxyl groups or water^{36,52} is more intense compared to that of the dry film. For the ppHMDSO film

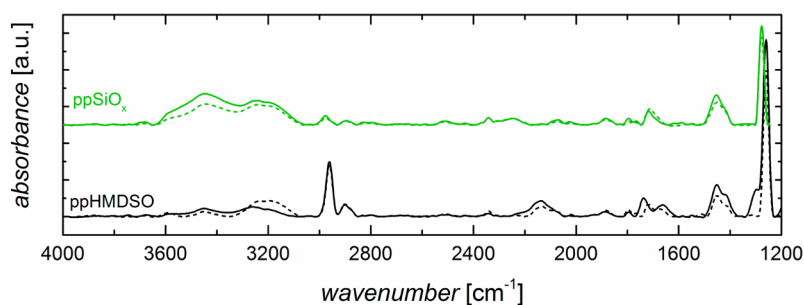


Figure 5. IR spectra of the ppSiO_x and ppHMDSO films after equilibration in water for 3 weeks at 20 °C (solid lines). The dry spectra are shown as references (dashed lines).

the intensity of the band around 3200 cm⁻¹ decreases slightly, which could be explained by secondary condensation reactions of silanols with water to form siloxane bonds.⁴⁴

The other regions of the spectra look very similar in the dry and in hydrated states. Slight increases in the CH_x vibrations around 1450 cm⁻¹ are observed. It is however not entirely clear whether those changes are due to changes within the films after equilibration in water or due to the large background generated by the broad Si–O–Si vibration band, which makes quantification difficult. Overall, the IR measurements of the hydrated films confirm the picture obtained from the neutron reflectometry study: The ppSiO_x film is effectively hydrated as shown by the increased intensity of the OH band attributed to water.

The differences seen for ppHMDSO are less obvious to interpret: The two methods used here have rather different sensitivities and resolutions toward vertical gradients: NR is sensitive to vertical changes in SDL on the order of less than 1 nm, while in the IR measurement the signal is averaged over micrometers, i.e., the complete thickness of the film. A comparably thin layer of different composition at the film surface does not strongly contribute to the total IR signal and may thus be overlooked. The films used for IR measurements were about 100 nm thick, i.e., roughly twice as thick as the films prepared for NR measurements. The absence of significant amounts of water in the IR spectrum for the hydrated ppHMDSO film therefore does not necessarily contradict the result of the neutron reflectivity study. We think it simply reflects that the IR measurement is done at its limit of sensitivity. Considering all above results, we can still conclude that both films must be hydrated, however not to the same extent.

The increase of scattering length density upon equilibration in heavy water observed in the reflectivity measurements may result from two simultaneous processes: (i) the observed penetration of D₂O into the film and (ii) the exchange of hydrogen by deuterium within the film. For the ppHMDSO film, a deuteration level of 6% can be expected according to the measurement by Nelson et al.¹⁸ in a similar film. For the ppSiO_x film, on the other hand, the level of proton exchange is not known. Thus, for this film two limiting cases can be considered: the maximal exchange of protons (i.e., all H atoms are replaced by D atoms) and a deuteration level equal to that of the ppHMDSO film. Assuming the exchange of all hydrogen atoms by deuterium, the NIST calculator⁵⁷ yields a scattering length density of $\rho_{\text{film,calcd}} = 3.60 \times 10^{-6} \text{ \AA}^{-2}$ for the ppSiO_x film. This SLD is lower than the value obtained from the best fit for the outermost layer ($\rho_{\text{film,measd}} = 3.88 \times 10^{-6} \text{ \AA}^{-2}$), suggesting that a significant amount of D₂O penetrates into the pores of this film.

Pore filling by water molecules in similar films has indeed already been observed by others.^{26,36,58} Using a volume fraction weighted addition¹⁸ of the film scattering length density ($\rho_{\text{film,calcd}}$) and the solvent scattering length density ($\rho_{\text{D}_2\text{O}}$) to explain the determined scattering length density ($\rho_{\text{film,measd}}$) gives a solvent volume fraction of about 10% in the outermost layer. A similar degree of solvent penetration was found for hydrophilic heptylamine plasma polymers.²⁷ For the other limiting case, i.e., when assuming a lower deuteration level of 6% for this film, a solvent volume fraction of about 25% in the outermost layer is obtained. Thus, the actual D₂O content in the outermost layer of the ppSiO_x film probably lies between these two limits. Further into the film, the SLD gradually decreases, indicating that less solvent reaches the deeper subsurface. The roughly 75 Å thick plasma polymer layer closest to the SiO₂ interface still shows the same SLD as in the dry state, revealing that the heavy water did not reach the substrate surface in significant amounts during the approximately 4 h incubation. Nevertheless, the water within the film is present not only at the film surface (top 2 nm of the film), but also in an extended subsurface region.

Increasing the temperature to 60 °C (i.e., decreasing the surface tension of D₂O) leads to an SLD increase of the inner sublayers of the ppSiO_x film, while the SLD near the film surface remains the same. However, the thickness of the outermost highly hydrated subsurface layer increases from 63 to 73 Å. The heavy water thus seems to penetrate further into the film, while all the accessible pores at the film surface are filled completely already at 20 °C. After reduction of the temperature again to 20 °C, a slight further increase in SLD in the deeper subsurface layers of the film is observed, indicating a further hydration of the film. The penetration of heavy water into the ppSiO_x film thus does not seem to be at equilibrium here, and the D₂O surface tension seems to play a minor role, while the time of exposure to the solvent appears to be an important factor.

On the other hand, for the ppHMDSO film a proton exchange of 6% was assumed according to Nelson et al.¹⁸ (i.e., 23 of the 379 H atoms were replaced by D atoms). The NIST calculator then yields a scattering length density of $\rho_{\text{film,calcd}} = 0.50 \times 10^{-6} \text{ \AA}^{-2}$ for the ppHMDSO film. This SLD is lower than the SLD of the outermost layer as determined by fitting ($\rho_{\text{film,measd}} = 0.59 \times 10^{-6} \text{ \AA}^{-2}$), suggesting that D₂O actually penetrates into the porous film. Also, this film swells slightly in an aqueous environment and thus indeed does not seem to be completely impermeable to water. Applying the volume fraction weighted addition of the solvent SLD ($\rho_{\text{D}_2\text{O}}$) and film SLD ($\rho_{\text{film,calcd}}$) to account for the observed SLD ($\rho_{\text{film,measd}}$) as described above then yields a solvent volume fraction of 2% within the outermost subsurface layer of the ppHMDSO film. This outermost layer extends over

about 6 nm in thickness, implying that also for the more hydrophobic ppHMDSO film water is present in the subsurface region. The increase in SLD upon an increase in temperature to 60 °C can be explained by a higher amount of solvent (5% in volume fraction) present within the film.

The similarity of the SLD profiles obtained at 20 °C before and after the heating cycle suggests that the D₂O penetration into the ppHMDSO film is essentially reversible. This reversibility can be attributed partly to the largely retained chain mobility of these films, which allows the methyl groups to optimize their orientation depending on the surrounding medium.^{59,60} The surface tension of the penetrating solvent thus is a factor determining hydration of this more hydrophobic film. However, the hydration equilibration time seems to be important for these films: in a previous study, it has been shown that the water contact angle measured after exposure to water for different time periods reaches its equilibrium value only after about 2 weeks in water.⁵ The volume fractions of water within the films obtained above can be transformed into changes in relative mass to quantitatively compare the results obtained by neutron reflectometry and ellipsometry. For the ppSiO_x and ppHMDSO films Δm_{rel} values of 5–13% and 1.6%, respectively, were calculated using the volume fractions of water in the outermost film layer obtained by NR compared to 2.2% and 0.25%, respectively, from the ellipsometry measurements. Within the error of estimation, both methods thus show a similar amount of water in/on the films.

Nevertheless, the kinetics seen are different in these experiments: the change in relative mass as determined by ellipsometry is nearly instantaneous and remains constant over a time period of 4 h, while the SLD profiles as determined by neutron reflectometry evolve with the exposure time to D₂O (i.e., more heavy water seems to penetrate into the films with time). In summary, these observations indicate that a quantitatively similar amount of water is taken up by the plasma polymer films as evidenced by ellipsometry and NR, but the kinetics are very different. We therefore conclude that the ellipsometer data show differences in surface condensation whereas the NR data clearly indicate water penetration into the plasma polymer film.

The diffusion of water in plasma polymer networks containing siloxane bonds is concentration dependent due to the hydrolysis of Si–O–Si bonds, and it follows a diffusion reaction mechanism described by Doremus.²⁵ Under the assumption that the concentration of the so-formed silanol groups inside the films is directly proportional to the local concentration of molecular water within the film, c , this model yields a concentration profile that exponentially decreases with the distance from the film surface for a system approaching equilibrium (see the [Supporting Information](#) for more details). Assuming that the change in scattering length density upon penetration of D₂O is directly proportional to the concentration of heavy water in the films, i.e., $\Delta\rho = \rho_{\text{film,meas}} - \rho_{\text{dry}} \propto c$, this model can be applied to explain the observed SLD profiles. Thus, for each layer in the models $\Delta\rho$ was calculated and plotted as a function of the distance from the surface. Thereby, the “position” of each layer was taken as its midpoint; e.g., the position of the outermost subsurface layers was set to be 31.5 Å, a half layer width less than the full thickness. [Figure 6](#) shows the so-obtained excess scattering for the hydrated ppHMDSO and ppSiO_x, respectively, relative to their dry states, measured at 20 °C, including the fit according to the model described above.

The excess scattering length reveals a nonlinear gradient, which indicates that hydration does not proceed via the linear

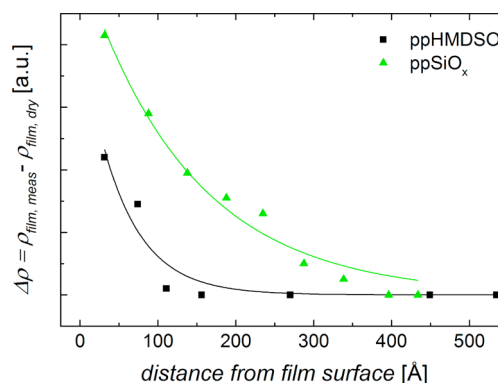


Figure 6. Excess scattering length density, $\Delta\rho$, as a function of the inward distance from the film surface for the ppSiO_x and ppHMDSO films. The lines are fits to the data using an exponentially decreasing function according to ref 25.

Fick law. A good agreement is obtained between the data and the proposed diffusion reaction mechanism, which can describe the diffusion of water into the ppHMDSO and ppSiO_x plasma polymer films. We think that water reacts with the siloxane network within the film to form more hydrophilic silanol groups that promote further penetration into the films. It is thus not surprising that the outermost surface of the nominally hydrophobic ppHMDSO film does not remain impermeable to water. Indeed, even PDMS is known to swell in water at equilibrium, albeit at extended equilibration times,⁶¹ suggesting that the water penetration depth in ppHMDSO plasma polymers might increase even further on a time scale of several weeks. Therefore, even in the more hydrophobic ppHMDSO film, water is present not only at the very surface (top 1–2 nm), but also as subsurface water reaching about 15 nm in depth ([Figure 6](#)).

Significantly thicker films of ppHMDSO can thus serve as kinetic barrier layers against water penetration. Thinner films, on the other hand, can be moderately hydrated and might thus exhibit interesting kinetics for applications such as drug release, protein adsorption, and biosensing. Note that, for both films, the slight gradient initially observed in the dry state might additionally facilitate solvent penetration into the films. Previously published results of a silver release study through such films (~100 nm thick) are in agreement with the above picture: no significant amount of silver is released through the ppHMDSO film (i.e., the water necessary to leach silver ions from the silver layer underneath does not reach the silver layer within the time frame of the experiment), while for the ppSiO_x film a considerable amount of silver is detected already after 1 day in water.⁵

4. CONCLUSION

The chemical structure and hydration behavior of two siloxane-based plasma polymer films were characterized using neutron reflectometry and complementary IR measurements. In the dry state, for both films an intrinsic minor density gradient perpendicular to the surface was observed. Seen as a whole, the more hydrophobic ppHMDSO film was shown to exhibit PDMS-like characteristics, while the more hydrophilic ppSiO_x film possesses a more inorganic nature and exhibits a higher neutron scattering length density. The behavior of the films in aqueous environments was investigated using in situ neutron reflectometry in D₂O at different temperatures. Characteristic SLD profiles reflecting film hydration could be extracted for each

film. Both films are hydrated: water penetrates into the nanoporous ppSiO_x film, reaching deep subsurface regions, while in the nominally hydrophobic ppHMDSO film the water reaches subsurface regions in a maximum depth of 10–15 nm. This latter film is thus not completely impermeable to water. The amount of water diffusing into the films depends on the chemical structure of the plasma polymer film and was found to be around 1–2% for the ppHMDSO film (in the respective outermost layer) and 5–13% for the ppSiO_x film, while a minority fraction of the signal can be due to deuterium exchange at siloxane groups. The extent of water penetration into the ppHMDSO film seems to depend on the surface tension of the penetrating aqueous solution and exhibits a reversible temperature effect. For both films, the diffusion of water into the films can be explained by a partly reversible reaction diffusion mechanism, where silanol groups are created along the siloxane network within the film upon reaction with water.

■ ASSOCIATED CONTENT

● Supporting Information

The Supporting Information is available free of charge on the ACS Publications website at DOI: [10.1021/acs.langmuir.5b03010](https://doi.org/10.1021/acs.langmuir.5b03010).

Reduced χ^2 values of the fits using the proposed models, fits of neutron reflectivity data using models with fewer layers, resulting in unsatisfying agreement between the fit and data, IR spectra including the broad Si–O–Si vibration, and excess scattering length densities for the measurements at 60 and 20 °C (PDF)

■ AUTHOR INFORMATION

Corresponding Author

*E-mail: manfred.heuberger@empa.ch.

Notes

The authors declare no competing financial interest.

■ ACKNOWLEDGMENTS

This work is based on experiments performed at the Swiss Spallation Neutron Source (SINQ), Paul Scherrer Institut, Villigen, Switzerland. The financial support by the Swiss National Science Foundation (Project No. 200021_134805) is gratefully acknowledged.

■ REFERENCES

- (1) Wrobel, A. M.; Wertheimer, M. R. Plasma-polymerized organosilicones and organometallics. In *Plasma Deposition, Treatment, and Etching of Polymers*; d'Agostino, R., Ed.; Academic Press: San Diego, CA, 1990; pp 163–268.
- (2) Choudhury, A. J.; Barve, S. A.; Chutia, J.; Pal, A. R.; Kishore, R.; Jagannath; Pande, M.; Patil, D. S. RF-PACVD of water repellent and protective HMDSO coatings on bell metal surfaces: Correlation between discharge parameters and film properties. *Appl. Surf. Sci.* **2011**, *257*, 8469–8477.
- (3) Hegemann, D.; Korner, E.; Blanchard, N.; Drabik, M.; Guimond, S. Densification of functional plasma polymers by momentum transfer during film growth. *Appl. Phys. Lett.* **2012**, *101*, 211603 (4p).
- (4) Hegemann, D. Plasma polymer deposition and coatings on polymers. In *Comprehensive Materials Processing*; Cameron, D., Ed.; Elsevier Ltd.: Oxford, U.K., 2014; Vol. 4, pp 201–228.
- (5) Blanchard, N. E.; Hanselmann, B.; Drost, J.; Heuberger, M.; Hegemann, D. Densification and hydration of HMDSO plasma polymers. *Plasma Processes Polym.* **2015**, *12*, 32–41.

(6) Gengenbach, T. R.; Chatelier, R. C.; Griesser, H. J. Correlation of the nitrogen 1s and oxygen 1s XPS binding energies with compositional changes during oxidation of ethylene diamine plasma polymers. *Surf. Interface Anal.* **1996**, *24*, 611–619.

(7) Menzies, D. J.; Nelson, A.; Shen, H.-H.; McLean, K. M.; Forsythe, J. S.; Gengenbach, T.; Fong, C.; Muir, B. W. An X-ray and neutron reflectometry study of PEG-like plasma polymer films. *J. R. Soc., Interface* **2012**, *9*, 1008–1019.

(8) Rau, C.; Kulisch, W. Mechanisms of plasma polymerization of various silico-organic monomers. *Thin Solid Films* **1994**, *249*, 28–37.

(9) Saulou, C.; Despax, B.; Raynaud, P.; Zanna, S.; Seyeux, A.; Marcus, P.; Audinot, J.-N.; Mercier-Bonin, M. Plasma-mediated nanosilver-organosilicon composite films deposited on stainless steel: Synthesis, surface characterization, and evaluation of antiadhesive and antimicrobial properties on the model yeast *saccharomyces cerevisiae*. *Plasma Processes Polym.* **2012**, *9*, 324–338.

(10) Alissawi, N.; Peter, T.; Strunskus, T.; Ebbert, C.; Grundmeier, G.; Faupel, F. Plasma-polymerized HMDSO coatings to adjust the silver ion release properties of Ag/polymer nanocomposites. *J. Nanopart. Res.* **2013**, *15*, 1–12.

(11) Xiangli, F.; Chen, Y.; Jin, W.; Xu, N. Polydimethylsiloxane (PDMS)/ceramic composite membrane with high flux for pervaporation of ethanol-water mixtures. *Ind. Eng. Chem. Res.* **2007**, *46*, 2224–2230.

(12) Guermat, N.; Bellel, A.; Sahli, S.; Segui, Y.; Raynaud, P. Thin plasma-polymerized layers of hexamethyldisiloxane for humidity sensor development. *Thin Solid Films* **2009**, *517*, 4455–4460.

(13) Nouicer, I.; Sahli, S.; Kihel, M.; Ziari, Z.; Bellel, A.; Raynaud, P. Superhydrophobic surface produced on polyimide and silicon by plasma enhanced chemical vapour deposition from hexamethyldisiloxane precursor. *Int. J. Nanotechnol.* **2015**, *12*, 597–607.

(14) Zanini, S.; Bami, R.; Pergola, R. D.; Riccardi, C. Development of super-hydrophobic PTFE and PET surfaces by means of plasma processes. *J. Phys.: Conf. Ser.* **2014**, *550*, 012029.

(15) Bieder, A.; Gruniger, A.; von Rohr, R. Deposition of SiO_x diffusion barriers on flexible packaging materials by PECVD. *Surf. Coat. Technol.* **2005**, *200*, 928–931.

(16) Hegemann, D.; Schuetz, U.; Oehr, C. RF-plasma deposition of SiO_x and a-C:H as barrier coatings on polymers. In *Plasma Processes and Polymers*; d'Agostino, R., Favia, P., Oehr, C., Wertheimer, M. R., Eds.; Wiley-VCH Verlag GmbH & Co. KGaA: Weinheim, Germany, 2005; pp 23–37.

(17) Foroughi Mobarakeh, L.; Jafari, R.; Farzaneh, M. Superhydrophobic surface elaboration using plasma polymerization of hexamethyldisiloxane (HMDSO). *Adv. Mater. Res.* **2011**, *409*, 783–787.

(18) Nelson, A.; Muir, B. W.; Oldham, J.; Fong, C.; McLean, K. M.; Hartley, P. G.; Oiseth, S. K.; James, M. X-ray and neutron reflectometry study of glow-discharge plasma polymer films. *Langmuir* **2006**, *22*, 453–458.

(19) Duncan, B.; Urquhart, J.; Roberts, S. *Review of Measurement and Modelling of Permeation and Diffusion in Polymers*; National Physical Laboratory: Middlesex, U.K., 2005.

(20) Russell, S.; Weinkauff, D. Vapor sorption in plasma polymerized vinyl acetate and methyl methacrylate thin films. *Polymer* **2001**, *42*, 2827–2836.

(21) Favre, E.; Schaetzel, P.; Nguyen, Q.; Clément, R.; Néel, J. Sorption, diffusion and vapor permeation of various penetrants through dense poly(dimethylsiloxane) membranes: a transport analysis. *J. Membr. Sci.* **1994**, *92*, 169–184.

(22) Watson, J.; Baron, M. The behaviour of water in poly(dimethylsiloxane). *J. Membr. Sci.* **1996**, *110*, 47–57.

(23) Tsigie, M.; Grest, G. Interdiffusion of solvent into glassy polymer films: A molecular dynamics study. *J. Chem. Phys.* **2004**, *121*, 7513–7519.

(24) Doremus, R. H. Diffusion of water in crystalline and glassy oxides: Diffusion-reaction model. *J. Mater. Res.* **1999**, *14*, 3754–3758.

(25) Doremus, R. H. Diffusion of water in silica glass. *J. Mater. Res.* **1995**, *10*, 2379–2389.

- (26) Erlat, A. G.; Spontak, R. J.; Clarke, R. P.; Robinson, T. C.; Haaland, P. D.; Tropsha, Y.; Harvey, N. G.; Vogler, E. A. SiO_x gas barrier coatings on polymer substrates: Morphology and gas transport considerations. *J. Phys. Chem. B* **1999**, *103*, 6047–6055.
- (27) Muir, B. W.; Nelson, A.; Fairbrother, A.; Fong, C.; Hartley, P. G.; James, M.; McLean, K. M. A comparative X-Ray and neutron reflectometry study of plasma polymer films containing reactive amines. *Plasma Processes Polym.* **2007**, *4*, 433–444.
- (28) Jeon, H.; Wyatt, J.; Harper-Nixon, D.; Weinkauff, D. Characterization of thin polymer-like films formed by plasma polymerization of methylmethacrylate: A neutron reflectivity study. *J. Polym. Sci., Part B: Polym. Phys.* **2004**, *42*, 2522–2530.
- (29) Hegemann, D.; Koerner, E.; Guimond, S. Macroscopic approach to investigate plasma polymer growth. *53rd Annu. Technol. Conf. Proc. - Soc. Vac. Coaters* **2010**, *17–22*, 409–413.
- (30) Clemens, D.; Gross, P.; Keller, P.; Schlumpf, N.; Koennecke, M. AMOR - the versatile reflectometer at SINQ. *Phys. B* **2000**, *276–278*, 140–141.
- (31) Parratt, L. G. Surface studies of solids by total reflection of X-Rays. *Phys. Rev.* **1954**, *95*, 359–369.
- (32) Braun, C. Parratt32, version 1.6.0, build 242, 2002.
- (33) Liu, H.-B.; Venkataraman, N. V.; Bauert, T. E.; Textor, M.; Xiao, S.-J. Multiple transmission-reflection infrared spectroscopy for high-sensitivity measurement of molecular monolayers on silicon surfaces. *J. Phys. Chem. A* **2008**, *112*, 12372–12377.
- (34) Sellmeier, W. Zur Erklärung der abnormen Farbenfolge im Spectrum einiger Substanzen. *Ann. Phys.* **1871**, *219*, 272–282.
- (35) Hegemann, D.; Brunner, H.; Oehr, C. Plasma Treatment of Polymers to Generate Stable, Hydrophobic Surfaces. *Plasmas Polym.* **2001**, *6*, 221–235.
- (36) Goulet, A.; Vallee, C.; Granier, A.; Turban, G. Optical spectroscopic analyses of OH incorporation into SiO₂ films deposited from O₂/tetraethoxysilane plasmas. *J. Vac. Sci. Technol., A* **2000**, *18*, 2452–2458.
- (37) Kiessig, H. Interferenz von Roentgenstrahlen an duennen Schichten. *Ann. Phys.* **1931**, *402*, 769–788.
- (38) Russell, T. X-ray and neutron reflectivity for the investigation of polymers. *Mater. Sci. Rep.* **1990**, *5*, 171–271.
- (39) Hillborg, H.; Ankner, J.; Gedde, U.; Smith, G.; Yasuda, H.; Wikström, K. Crosslinked polydimethylsiloxane exposed to oxygen plasma studied by neutron reflectometry and other surface specific techniques. *Polymer* **2000**, *41*, 6851–6863.
- (40) Grimoldi, E.; Zanini, S.; Siliprandi, R. A.; Riccardi, C. AFM and contact angle investigation of growth and structure of pp-HMDSO thin films. *Eur. Phys. J. D* **2009**, *54*, 165–172.
- (41) Siliprandi, R.; Zanini, S.; Grimoldi, E.; Fumagalli, F.; Barni, R.; Riccardi, C. Atmospheric pressure plasma discharge for polysiloxane thin films deposition and comparison with low pressure process. *Plasma Chem. Plasma Process.* **2011**, *31*, 353–372.
- (42) Zabel, H. X-ray and neutron reflectivity analysis of thin films and superlattices. *Appl. Phys. A: Solids Surf.* **1994**, *58*, 159–168.
- (43) Yasuda, H.; Hsu, T. Some aspects of plasma polymerization investigated by pulsed R.F. discharge. *J. Polym. Sci., Polym. Chem. Ed.* **1977**, *15*, 81–97.
- (44) Wrobel, A. M. Aging process in plasma-polymerized organo-silicon thin films. *J. Macromol. Sci., Chem.* **1985**, *22*, 1089–1100.
- (45) Despax, B.; Raynaud, P. Deposition of “polysiloxane” thin films containing silver particles by an RF asymmetrical discharge. *Plasma Processes Polym.* **2007**, *4*, 127–134.
- (46) Launer, P. J. *Infrared Analysis of Organosilicon Compounds: Spectra-Structure Correlations*; Technical Report for Petrarch Systems, Bristol, PA, 1987; pp 100–103.
- (47) Burke, D. D.; Gleason, K. K. Structure and mechanical properties of thin films deposited from 1,3,5-trimethyl-1,3,5-trivinylcyclotrisiloxane and water. *J. Appl. Phys.* **2003**, *93*, 5143–5150.
- (48) Anderson, R.; Arkles, B.; Larson, G. *Silicon Compounds Review and Register*; Technical Report for Petrarch Systems, Bristol, PA, 1987.
- (49) Lucovsky, G. Chemical effects on the frequencies of Si-H vibrations in amorphous solids. *Solid State Commun.* **1979**, *29*, 571–576.
- (50) Aumaille, K.; Vallée, C.; Granier, A.; Goulet, A.; Gaboriau, F.; Turban, G. A comparative study of oxygen/organosilicon plasmas and thin SiO_xCyHz films deposited in a helicon reactor. *Thin Solid Films* **2000**, *359*, 188–196.
- (51) Fanelli, F.; Lovascio, S.; d'Agostino, R.; Arefi-Khonsari, F.; Fracassi, F. Ar/HMDSO/O₂ fed atmospheric pressure DBDs: Thin film deposition and GC-MS investigation of by-products. *Plasma Processes Polym.* **2010**, *7*, 535–543.
- (52) Pliskin, W. A. Comparison of properties of dielectric films deposited by various methods. *J. Vac. Sci. Technol.* **1977**, *14*, 1064–1081.
- (53) Fang, J.; Chen, H.; Yu, X. Studies on plasma polymerization of hexamethyldisiloxane in the presence of different carrier gases. *J. Appl. Polym. Sci.* **2001**, *80*, 1434–1438.
- (54) Wavhal, D. S.; Zhang, J.; Steen, M. L.; Fisher, E. R. Investigation of gas phase species and deposition of SiO₂ films from HMDSO/O₂ plasmas. *Plasma Processes Polym.* **2006**, *3*, 276–287.
- (55) Zanini, S.; Riccardi, C.; Orlandi, M.; Esena, P.; Tontini, M.; Milani, M.; Cassio, V. Surface properties of HMDSO plasma treated polyethylene terephthalate. *Surf. Coat. Technol.* **2005**, *200*, 953–957.
- (56) Li, K.; Gabriel, O.; Meichsner, J. Fourier transform infrared spectroscopy study of molecular structure formation in thin films during hexamethyldisiloxane decomposition in low pressure rf discharge. *J. Phys. D: Appl. Phys.* **2004**, *37*, 588–594.
- (57) <http://www.ncnr.nist.gov/resources/activation/> (accessed May 2014).
- (58) Guermat, N.; Bellel, A.; Sahli, S.; Segui, Y.; Raynaud, P. Water molecule sensitive layers deposited from hexamethyldisiloxane/oxygen mixture at low temperature. *Mater. Sci. Forum* **2009**, *609*, 69–73.
- (59) Gengenbach, T. R.; Griesser, H. J. Post-deposition ageing reactions differ markedly between plasma polymers deposited from siloxane and silazane monomers. *Polymer* **1999**, *40*, 5079–5094.
- (60) Siderakis, K.; Pylarinos, D. Room temperature vulcanized silicone rubber coatings: Application in high voltage substations. In *Concise Encyclopedia of High Performance Silicones*; Tiwari, A., Soucek, M. D., Eds.; John Wiley & Sons, Inc.: Hoboken, NJ, 2014; pp 1–17.
- (61) Yang, H.; Nguyen, Q. T.; Ding, Y.; Long, Y.; Ping, Z. Investigation of poly(dimethyl siloxane) (PDMS)-solvent interactions by DSC. *J. Membr. Sci.* **2000**, *164*, 37–43.